

Green's function-based control-oriented modeling of electric field for dielectrophoresis

Martin Gurtner,^{1, a)} Kristian Hengster-Movric,¹ and Zdeněk Hurák^{1, b)}

Faculty of Electrical Engineering, Czech Technical University in Prague,
Czech Republic.

(Dated: 3 December 2024)

In this paper, we propose a novel approach to obtaining a reliable and simple mathematical model of a dielectrophoretic force for feedback micromanipulation. Any such model is expected to sufficiently accurately relate the voltages (electric potentials) applied to the electrodes with the resulting forces exerted on microparticles at given locations. This model also has to be computationally simple enough to be used in real time as required by feedback control. Most existing models involve solving two- or three-dimensional mixed boundary value problems. As such, they are usually analytically intractable and have to be solved numerically. A numerical solution is infeasible in real time hence such models are not at all suitable for feedback control. We present a novel approximation of the boundary value data for which a closed-form analytical solution is feasible; we solve a mixed boundary value problem numerically off-line and only once, and based on this solution we approximate the mixed boundary conditions by Dirichlet boundary conditions. This way we get an approximated boundary value problem for which the analytical framework of Green's functions is applicable. Thus obtained closed-form analytical solution is amenable to real-time use and closely matches the numerical solution of the original exact problem.

Keywords: dielectrophoresis, micromanipulation, Green's function

I. INTRODUCTION

Since its invention by H. Pohl in the 1950s and 1960s^{1,2}, *dielectrophoresis (DEP)* has proved an efficient tool for transportation, separation, and characterization of microparticles such as e.g. biological cells (see Refs. 3 and 4 for a recent survey and comprehensive introduction). More often than not, DEP is used to manipulate ensembles of large numbers of microparticles. However, recently some attempts were successful to use DEP in a feedback control scheme for a high accuracy noncontact manipulation of a single microparticle^{5–8}; these developments can be viewed as a reopening of the topic first started in the 1990s⁹. The technology has also boosted development in this area; there are reported CMOS chips integrating both actuation and sensing and thus enabling individual and independent manipulation of thousands of cells¹⁰. This technology has later been commercialized by Silicon Biosystems as a commercial product called DEPArray. These non-contact tweezers are usually based on a feedback control scheme, typically invoking an automatic visual tracking. The feedback control, in turn, requires a sufficiently accurate mathematical model of the underlying physical phenomenon of DEP. The relationship between the voltages applied to the microelectrodes and the DEP force exerted on a microparticle located at a given position needs to be evaluated periodically as the microparticle moves around the workspace. Sampling periods on a time-scale of few tens of milliseconds or even a few milliseconds are not unusual. The commonly used approaches to modeling DEP—which are based on numerical solution of the corresponding *Boundary Value Problem (BVP)*, typically using *Finite Elements Method (FEM)* or *Method of Moments (MOM)*—are not feasible in real time. It is

^{a)} Electronic mail: martin.gurtner@fel.cvut.cz

^{b)} <http://aa4cc.dce.fel.cvut.cz>.

possible to precompute and store these solutions in a computer memory (as reported in Ref. 5) but this approach imposes stringent requirements on the volume of data stored. There are approaches described in the literature that provide analytical solutions^{11–13}; they are, however, only usable for simple electrode arrays and fixed harmonic voltage signals applied to the electrodes while the feedback control requires the ability to change the voltages in real time.

In this paper, we propose a modeling methodology that provides a computationally simple yet sufficiently accurate model of a DEP force for the purposes of feedback micromanipulation. In the proposed methodology, we combine a numerical and analytical approach to the modeling of DEP. Existing models of DEP usually involve a numerical solution of an analytically intractable *mixed Boundary Value Problem* (*mBVP*) for the potential. As the numerical solution is infeasible in real time and might be too large for storing in a computer memory, it is desirable to find a closed-form approximate analytical expression for the potential. To find such an expression, we solve numerically the original *mBVP*. Based on this numerical solution, we approximate the *mBVP* by a *BVP* for which the closed-form solution can be found by the framework of Green's functions. Using the approximate closed-form expression for the potential we obtain a model of DEP force that is computationally effective and requires almost no memory space. The numerical solution of the *mBVP* is computed off-line and only once. Thus the high computational burden associated with the numerical solution is carried out off-line and the feedback control system uses only the approximate closed-form analytical solution in real time.

The paper is organized as follows. In Section II, we briefly present the commonly used dipole model of DEP and show what prevents its direct use in feedback micromanipulation. In Section III we propose a control-oriented model derived from the dipole model by Green's functions. Experimental verification of the viability of the proposed model is provided in Section IV. Conclusions are given in Section V.

II. FEEDBACK MANIPULATION BY DIELECTROPHORESIS

A great advantage of feedback manipulation by DEP, in contrast to the conventional use of DEP, is that it allows one to manipulate individual microparticles. Nevertheless, this comes with the cost of higher computational demands on the control system because the voltages applied to the electrodes cannot be precomputed anymore and have to be adjusted in real time as required by the feedback loop.

We can explain this with an aid of Fig. 1 depicting the scheme of feedback manipulation by DEP. The measured position of the microparticle is subtracted from the required position. The deviation is fed to a control system that calculates a DEP force needed to lower this deviation—to steer the microparticle towards the required position. Therefore, the voltages on electrodes are required to generate such a force. Such voltages are then applied to the electrodes and a generated DEP force acts on the microparticle moving it towards the required position. The new position is measured and the whole cycle is repeated. The crucial part of this algorithm is hidden in the control system where, in order to compute the voltages generating the desired DEP force, a model relating the voltages to the DEP force has to be used in real time.

Nevertheless, exact DEP models are rather complicated to use in real time. For instance, the widely used *dipole model* has the following form: time-averaged dielectrophoretic force acting on a homogeneous spherical particle in a sinusoidal field is¹⁴

$$\begin{aligned} \langle \mathbf{F}_{\text{DEP}}(t) \rangle = \pi \varepsilon_m r^3 & \left(\text{Re}\{K(\omega)\} \nabla |\mathbf{E}|^2 + 2\text{Im}\{K(\omega)\} \right. \\ & \left. \times (E_x^2 \nabla \varphi_x + E_y^2 \nabla \varphi_y + E_z^2 \nabla \varphi_z) \right), \end{aligned} \quad (1)$$

where ε_m is the permittivity of surrounding medium, r is the particle's radius, $K(\omega)$ is a frequency dependent constant known as Clausius–Mossotti factor, $\mathbf{E} = [E_x, E_y, E_z]$ is the amplitude of the harmonic electric field $\text{Re}\{\mathbf{E} e^{i\omega t}\}$, the phase of the electric field is denoted by φ_a , $a \in \{x, y, z\}$ and finally, $\text{Re}\{\cdot\}$ and $\text{Im}\{\cdot\}$ denote real and imaginary parts

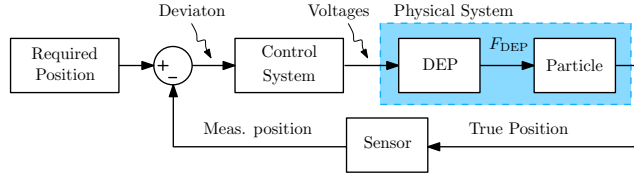


FIG. 1. A block diagram of feedback manipulation by DEP.

of a complex number, respectively. For brevity, the spatial dependence is omitted in the notation.

According to (1), to determine the DEP force due to applied voltages to electrodes, one needs to know the electric field \mathbf{E} . The electric field \mathbf{E} is given by $\mathbf{E} = -\nabla\phi$, where the potential ϕ is calculated from Laplace equation $\nabla^2\phi = 0$ with mixed boundary conditions. Orienting the reference frame so that the electrodes lie in the x - y plane and manipulated objects are situated above it, the domain is defined by the half-space $z > 0$. The boundary conditions are given by the voltages applied to the electrodes (Dirichlet boundary condition) and a zero-flux condition in the normal direction to the electrode plane in the intervening space between the electrodes (Neumann boundary condition)¹¹. This BVP is analytically intractable and can be solved only approximately by numerical solvers. Since the control algorithm is supposed to run in real time and the calculation of the DEP force must not take more than a few milliseconds, solving on-line this exact BVP numerically is infeasible.

A partial remedy to this issue is to express explicitly the dependence of \mathbf{F}_{DEP} on the voltages applied to the electrodes. By superposition, we express the net potential $\phi(x, y, z)$ as a weighted sum of normalized contributions from individual electrodes. That is,

$$\phi(x, y, z) = \sum_{i=1}^n u_i \phi_i(x, y, z), \quad (2)$$

where n is the number of electrodes, u_i serves as a scaling factor given by voltage on i th electrode, ϕ_i is the contribution to the net potential from the i th electrode when 1V is applied to it, and the remaining electrodes are grounded. Now, to determine the net potential $\phi(x, y, z)$, we have to solve n BVPs ($\nabla^2\phi_i = 0$, $i = 1, \dots, n$) that are still analytically intractable, but that do not change with the voltages applied to the electrodes.

One can solve each of these BVPs numerically on a grid of points in advance, store the solution and use it as a look-up table in real time. Nevertheless, this look-up table grows unacceptably large. As an example, let the microparticles be manipulated within an area of size $1500 \times 1500 \times 300 \mu\text{m}$. If we grid this area equidistantly with points separated by $5 \mu\text{m}$, we obtain $300 \times 300 \times 60 = 5,400,000$ points. Naïve implementation of this approach would thus require to store $[E_x, E_y, E_z]$ and their partial derivatives $[\frac{\partial E_x}{\partial x}, \frac{\partial E_x}{\partial y}, \frac{\partial E_x}{\partial z}, \frac{\partial E_y}{\partial y}, \frac{\partial E_y}{\partial z}]$ for each point in order to evaluate \mathbf{F}_{DEP} and all that is only for one electrode.

The volume of the data needed to be stored can be reduced by a method introduced by Kharbouly et al.¹⁵. Instead of storing directly the derivatives of the potential in points spread throughout all the domain, they store precomputed surface charge density in a grid on electrodes. In real time, when there is a request to compute the DEP force at a point, they numerically integrate the precomputed surface charge density to calculate the electric field and its derivatives at that point and that allows to compute the DEP force. Nevertheless, for the previous case that still means that a large portion—depending on what extent of the electrode plane is occupied by the electrodes—of $300 \times 300 = 90,000$ points have to be stored. Furthermore, the reduction in the volume of data comes at the cost of higher computational complexity because all the stored data points are needed for evaluation of (1).

In this paper, we propose a different approach. We approximate the previously mentioned, analytically intractable boundary value data so that a closed-form approximated solution can be found.

III. GREEN'S FUNCTIONS FOR MODELING OF DIELECTROPHORESIS

The solution of the Laplace equation in a half-space domain, which is the case here, with Dirichlet conditions only can be transformed into an integration by use of the Green's theorem. The derivation can be found in Ref. 13 and the resulting formulas are

$$\phi(x, y, z) = \frac{z}{2\pi} \iint_{-\infty}^{\infty} \frac{h(x', y')}{[(x - x')^2 + (y - y')^2 + z^2]^{3/2}} dx' dy' \quad (3)$$

for a general 3D case and

$$\phi(x, z) = \frac{z}{\pi} \int_{-\infty}^{\infty} \frac{h(x')}{(x - x')^2 + z^2} dx' \quad (4)$$

for the 2D case where one axis, in our case y , is redundant, the letter the electrode array has infinitely long electrodes along that y axis. The function $h(x, y)$ and $h(x)$ represent values of $\phi(x, y, 0)$ and $\phi(x, 0)$, respectively, imposed by the Dirichlet boundary conditions. Thus, to obtain a closed-form description of the potential—and subsequently also of the DEP force—one only needs to compute the integral (3) or (4). However, in order to achieve that, it is necessary to know $h(x, y)$ (or $h(x)$) and that means also the potential in the electrode plane in the intermediate space between the electrodes where the mixed boundary conditions impose a zero normal flux.

To determine the values of the potential on the electrode plane in between the electrodes, linear^{11,12} or polynomial¹³ approximation of the decay of the potential away from the electrode can be found in the literature. Nevertheless, for more complex electrode array designs, integrals (3) and (4) are analytically intractable even for linear approximations and thus have to be solved numerically. Then, however, formulating the solution of the boundary value problem as an integration is meaningless since both the new and the original problem have to be solved numerically. In this paper, instead, we approximate the potential on the electrode plane so that integrals (3) or (4) are expressible in terms of elementary functions, thus providing a closed-form solution for the potential and consequently a closed-form solution for the DEP force. It is worth of note that since the potential—as the solution of the Laplace equation—is a harmonic function, it is infinitely differentiable¹⁶.

A. Example 1: Parallel Electrode Array

Let us consider the electrode array with single electrode width b , distance between the electrodes (center to center) d and $(2n + 1)$ electrodes (see Fig. 2(a)). We assume that the electrodes are infinitely long and thus drop the dependence on the y coordinate altogether.

We decompose the net potential by (2) to a weighted sum of normalized contributions ϕ_i from individual electrodes. Furthermore, we assume that the potential contribution ϕ_i is shift invariant for a shift d along the x -axis. That means the potential contribution ϕ_i is identical for each electrode up to a shift. Mathematically,

$$\phi_i(x, z) = \phi_{i\pm 1}(x \pm d, z), \quad i = -n + 1, \dots, n - 1. \quad (5)$$

Clearly, this assumption does not hold for the electrodes close to the edge of the electrode array. For instance, the potential contribution $\phi_n(x, z)$ (i.e. from the electrode on the edge) decays more quickly towards the $(n - 1)$ th electrode, which is grounded, than towards the other side, where there is no grounded plate near. To overcome this issue and to justify making assumption (5), we assume that it is possible to manufacture grounded plates along the perimeter.

As a result of assumption (5), we have to compute the integral (4) only for one $\phi_i(x, z)$, e.g. $\phi_0(x, z)$. The remaining potential contributions are determined simply by shifting, that is $\phi_i(x, z) = \phi_0(x + id, z)$ with $i \in \{-n, \dots, n\}$, and the net potential is then given

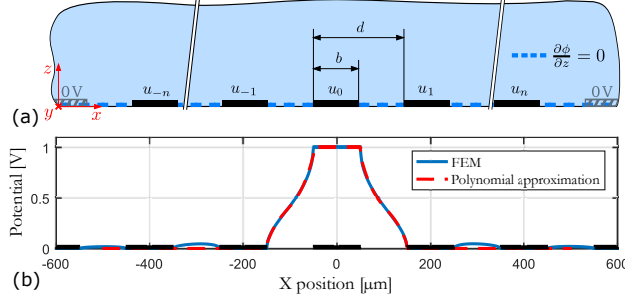


FIG. 2. Parallel electrode array: (a) a side-view diagram and (b) an approximation of the boundary conditions. The black rectangles represent electrodes and the shaded rectangles represent possibly added grounding plates.

by (2). Nevertheless, to compute (4) for $\phi_0(x, z)$, we need to know $h(x) := \phi_0(x, 0)$ while the values of $\phi_0(x, 0)$ are known only on the electrodes and unknown on the rest of the bottom boundary. To overcome this problem, we solve the original Laplace equation with mixed boundary conditions numerically by *Finite Element Method (FEM)* in COMSOL Multiphysics. Then, we take the values of the potential on the bottom boundary between the 0-th electrode and its left adjacent electrode and fit a polynomial $p(x)$ to these values. The polynomial approximation of $h(x)$ is

$$\tilde{h}(x) = \begin{cases} p(x) & x \in \left[-d - \frac{b}{2}, -\frac{b}{2}\right), \\ 1 & x \in \left[-\frac{b}{2}, \frac{b}{2}\right], \\ p(-x) & x \in \left(\frac{b}{2}, d + \frac{b}{2}\right], \\ 0 & \text{otherwise,} \end{cases} \quad (6)$$

Specifically, for an electrode array with parameters $d = 2b = 200 \mu\text{m}$, we fitted a third-order polynomial to the FEM solution and the fitted polynomial is

$$p(x) = 1.36 \cdot 10^{-6}x^3 + 4.34 \cdot 10^{-4}x^2 + 5.15 \cdot 10^{-2}x + 2.59 \quad (7)$$

where x is in micrometers.

The FEM solution together with the polynomial approximation is displayed in Fig. 2(b). Apparently, the polynomial approximation describes the FEM solution very accurately. However, one should not overlook the small humps in the gaps between the electrodes, which are completely omitted by the approximation.

With $\tilde{h}(x)$ approximating $\phi_0(x, 0)$ we can compute the integral (4) and obtain an approximate closed-form solution for $\phi_0(x, z)$. Then, by (5) and (2) we get the net potential $\phi(x, z)$ for any choice of electrode potentials u_i . Thus, we can compute the electric field intensity and the pertaining the DEP force. We do not present the evaluated integral here, because it is rather lengthy and it would not serve any purpose but It is crucial that this integral is expressible in terms of elementary functions.

To validate the proposed model, we compare DEP force fields computed by (1) for the potential obtained by numerical solution of the original boundary value problem with mixed boundary conditions and for the potential obtained by solution of the approximated boundary value problem. The comparison is shown in Fig. 3 (Multimedia view) . The comparison is carried out for an electrode array with nine electrodes ($n = 4$), with grounded perimeter (also visible in the figure) and with single electrode width $b = 100 \mu\text{m}$ and distance between the electrodes $d = 200 \mu\text{m}$. The remaining parameters are: $r = 25 \mu\text{m}$, $\epsilon_m = 7.08 \cdot 10^{-10} [\text{F}/\text{m}]$ and $K(\omega) = -0.4618 - 0.1454i$. As usual for standing wave DEP, the sinusoidal signal applied on all electrodes has the same frequency and phase. Since it is rather difficult to compare the vector fields, the comparison is done for one particular height above the electrodes ($120 \mu\text{m}$) and for varying potentials on the electrodes.

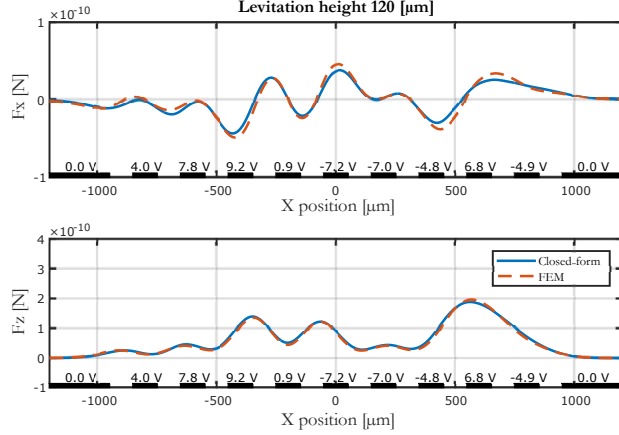


FIG. 3. A component-wise comparison of DEP force fields computed for parallel electrode array ($d = 2b = 200 \mu\text{m}$) numerically by FEM and analytically based on the approximate closed-form solution for the potential. The force fields are computed for height $120 \mu\text{m}$ above the electrode array. The applied potentials are shown above the electrodes represented by the black rectangles. (Multimedia view)

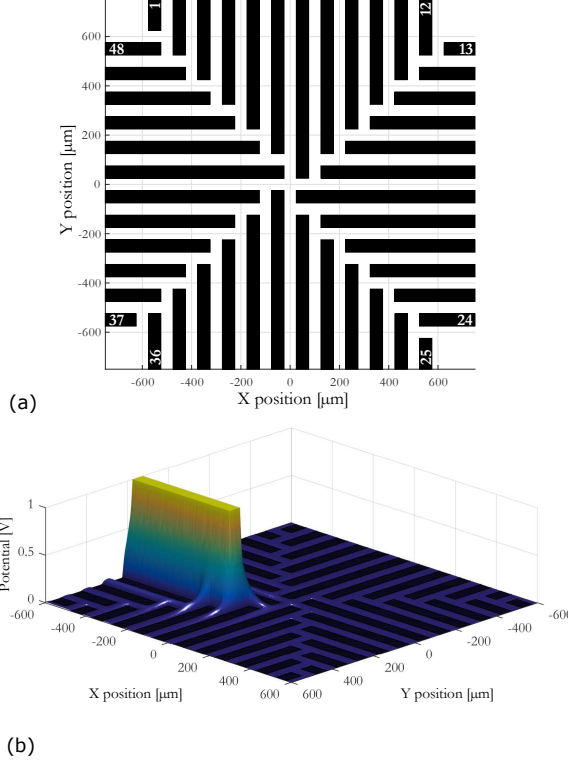


FIG. 4. Four-sector electrode array: (a) a top-view diagram and (b) FEM solution for the normalized potential contribution from one electrode.

B. Example 2: Four-sector Electrode Array

In the second example, we show a related approach how to approximate the values of the potential on the electrode plane for a more complex electrode array shown in Fig. 4(a). It consists of four sectors and allows manipulation of microparticles in all three directions

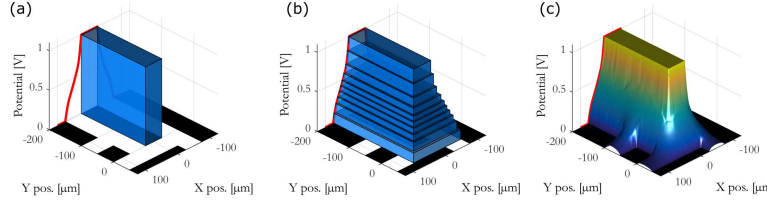


FIG. 5. An approximation of the desired shape of the bottom boundary condition for four-sector electrode array: (a) one block approximation, (b) staircase approximation and (c) boundary condition obtained by FEM. Black rectangles represent electrodes.

above the electrode array, as it was experimentally verified¹⁷. The width of the electrodes is $b = 50 \mu\text{m}$ and the distance between the electrodes (center to center) is $d = 100 \mu\text{m}$. We assume that the electrodes extend to infinity at one end.

Along similar lines as in Example 1, based on the superposition principle (2) we express the net potential as a weighted sum of normalized contributions ϕ_i from individual electrodes and make a similar assumption that the normalized contributions are identical up to a shift and/or rotation with respect to each other; for instance, for electrodes with indexes ranging from 1 to 7 (the indexes are shown in Fig. 4(a)), it holds that

$$\phi_{i+1}(x, y, z) = \phi_i(x - d, y + d, z), \quad (8)$$

where d is center-to-center distance between the electrodes.

Again, thanks to this assumption, we need to compute the integral (3) only for one $\phi_i(x, y, z)$. In this case, we choose $\phi_{44}(x, y, z)$ because it is close to the center of the sector and, analogously to the previous example, the assumption (8) holds best for the electrodes in the center.

It remains to find the approximation of $h(x, y) := \phi_{44}(x, y, 0)$. In order to do that, we approximate the FEM solution for $\phi_{44}(x, y, 0)$ shown in Fig. 4(b). This time, however, the integral (3) is analytically intractable for $h(x, y)$ being polynomial or even linear—we are unable to evaluate the integral for anything else than for a constant boundary condition. Thus, instead of using a polynomial or linear approximation, the desired shape of the potential is constructed from blocks. Initially, we approximate the boundary condition in the roughest possible way; we assume that the potential between the electrodes drops immediately to zero as one moves away from the electrode (see Fig. 5(a)). Then summing the “scaled” and “shifted” versions of this boundary condition (see Fig. 5(b)) approximately gives the desired shape (see Fig. 5(c)).

Let us begin with the one-block approximation. We define the block boundary condition for one-side infinitely long electrode as

$$h_0(x, y) = \begin{cases} 1 & x \leq 0 \text{ and } y \in \left[-\frac{b}{2}, \frac{b}{2}\right], \\ 0 & \text{otherwise,} \end{cases} \quad (9)$$

where b is the width of the electrode. The staircase approximation of the desired shape is then obtained by

$$\tilde{h}(x, y) = \sum_{i=1}^N \alpha_i h_0 \left(x - \frac{(\beta_i - 1)b}{2}, \frac{y}{\beta_i} \right), \quad (10)$$

where N is the number of blocks, α_i determines the height of the block and β_i is a scaling parameter, meaning that $\beta_i = 2$ scales the block so that it is twice as wide as the original electrode. Notice, that we assumed that the potential decays identically along the x and y axes and thus the coefficients β_i determine not only the width but simultaneously also the shift of the blocks along the x axis.

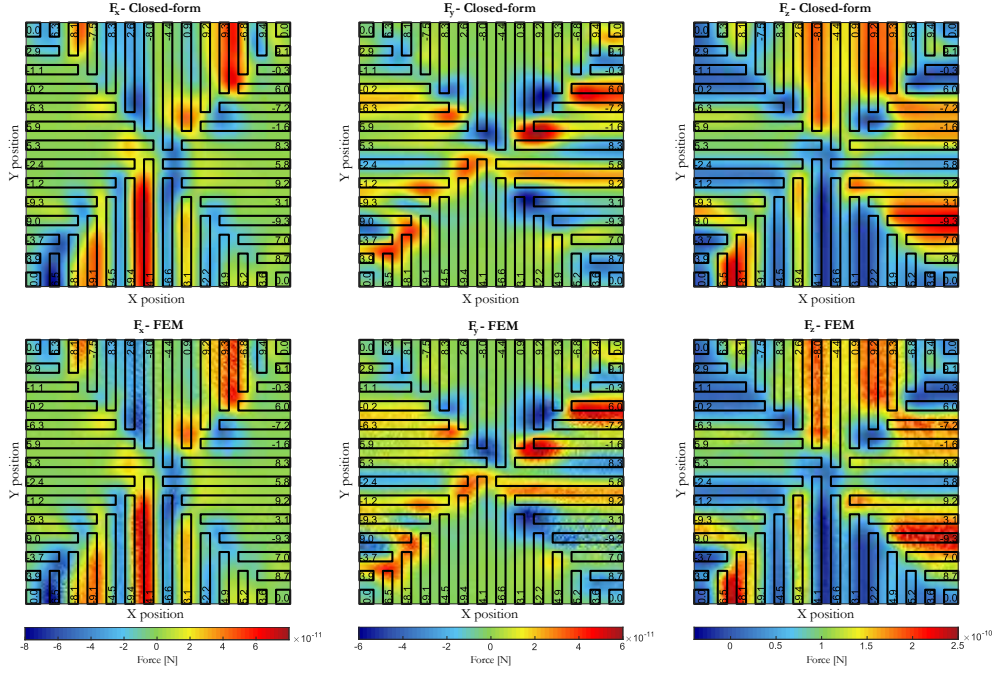


FIG. 6. A comparison of individual components of DEP force fields calculated for four-sector electrode array numerically by FEM and analytically based on the approximate closed-form solution for the potential. The force fields are computed for height 120 μm above the electrode array. The numerical values inside the electrodes represent applied potentials in volts. (Multimedia view)

Given the FEM solution, the coefficients α_i and β_i in (10) can be determined by solving the following optimization problem

$$\begin{aligned} \min_{\alpha_i, \beta_i \in \mathbb{R}, i=1, \dots, N} \quad & \|\tilde{h}(x_0, y) - \phi_{\text{FEM}}(x_0, y, 0)\|_2 \\ \text{subject to:} \quad & \sum_{i=1}^N \alpha_i = 1, \\ & \beta_i \in [1, 3], \quad i = 1, \dots, N, \end{aligned} \quad (11)$$

where $\phi_{\text{FEM}}(x, y, z)$ is the FEM solution. Note that the 2-norm above measures the size of a function of the real y variable, but in the numerical optimization we are only able to consider samples of y , which is not encoded in the optimization problem statement for the sake of simplicity. With the assumption that the potential decays identically along x and y axes, both α_i and β_i can be determined from a y - z cross-section of $\phi_{\text{FEM}}(x, y, 0)$, we fixed x to be a negative constant value x_0 . For instance, the red curve in Fig. 5(a) represents $\phi_{\text{FEM}}(x_0, y, 0)$ for $x_0 = -200 \mu\text{m}$. The coefficients α_i have to sum up to one because only then the height of the piled up blocks will be one. We restrict the coefficients β_i to the interval $[1, 3]$ because then the blocks cannot be narrower than the electrode and they cannot interfere with other electrodes. Even though the optimization task is not convex, it still provides very good results when given a good initial guess. For the initial guess, we let β_i to grow linearly from 1 to 3 and set α_i to be proportional to $\frac{\partial}{\partial y} \phi_{\text{FEM}}(x_0, y, 0)$. Figure 5(b) shows results of the optimization task for $N = 10$.

Having the approximation of the boundary condition $\tilde{h}(x, y)$, one can calculate the integral (3) and obtain a closed-form solution for $\phi_{44}(x, y, z)$. Instead of using the boundary condition $\tilde{h}(x, y)$ composed of several blocks, due to linearity of the integral, we can use the one-block boundary condition $h_0(x, y)$, calculate the integral (3) and compose the closed-form approximation for $\phi_{44}(x, y, z)$ in the same way as $\tilde{h}(x, y)$ is composed. This is exactly

how we proceed. Substitution of $h_0(x, y)$ to the integral (3) gives us

$$\phi_{i0}(x, y, z) = \frac{z}{2\pi} \int_{-\frac{b}{2}-\infty}^{\frac{b}{2}} \int_0^0 \frac{1}{((x-x')^2 + (y-y')^2 + z^2)^{3/2}} dx' dy'. \quad (12)$$

Again, we do not present the evaluated integral since one can easily compute it in Wolfram Mathematica, Maple, Matlab or yet another computer algebra package, but it is expressible in terms of elementary functions. The approximate closed-form solution for $\phi_{44}(x, y, z)$ is then obtained as

$$\phi_i(x, y, z) = \sum_{i=1}^N \alpha_i \phi_{i0} \left(x - \frac{(\beta_i - 1)b}{2}, \frac{y}{\beta_i}, z \right). \quad (13)$$

Similarly, as in the 2D case, we do not compare the potentials directly because what we are interested in are the DEP force fields derived from the potentials. Since it is a rather challenging task to compare 3D force fields, we compare their components separately. The comparisons were carried out for the same parameters as in Example 1 and they are shown in Fig. 6 (Multimedia view). Fig. 6 shows a comparison carried for randomly varying potentials on the electrodes. Based on the comparison, the force field computed from the approximate solution matches the force field based on the FEM solution.

IV. EXPERIMENTAL VERIFICATION

To verify the applicability of the proposed DEP model, we used it in an experiment with 50 μm polystyrene microsphere was manipulated by a control system with a feedback loop. The goal of the control system is to steer the microparticle along a reference trajectory. The microsphere was suspended in water contained in a pool above a parallel electrode array with six electrodes and $d = 2b = 200 \mu\text{m}$ (see Fig. 2(a)). A detailed description of the control system can be found in Ref. 5. Figure 7 shows reference and measured trajectories of the microparticle. In addition, the figure also displays what potentials had to be applied in time to the electrodes in order to steer the microparticle along the reference trajectory. These potentials were computed in real time by the control system based on the proposed DEP model. It is noteworthy, that in Ref. 5 numerical solution taking approximately 1 GB of space was used to calculate DEP force in real time, whereas here the DEP model is represented by a closed-form analytical expression that is easily evaluable and take almost no memory space.

V. CONCLUSION

Although the presented approach to modeling of dielectrophoresis is demonstrated on the dipole approximation of the microparticles, it can also be applied to more complex and accurate multipole approximations; no modification would be needed because multipole approximations only require higher derivatives of the potential and our proposed approximation calculates an infinitely differentiable closed-form approximation of the potential. Even though we demonstrate the approach on two concrete electrode array designs, it can also be used for other planar designs exhibiting similar symmetry; two such examples are shown in Fig. 8. Note that full analytical solutions for exact boundary conditions are not possible in such cases.

The major benefit of our approximate modeling methodology for a dielectrophoretic force presented here is that in comparison with the standard FEM-based (or other numerical) approaches it yields a mathematical model whose use is feasible in real time (e.g. in cycles of every few milliseconds or so) on a common laboratory PC, and yet the accuracy of the model is sufficient for the purposes of feedback micromanipulation. The approach is particularly

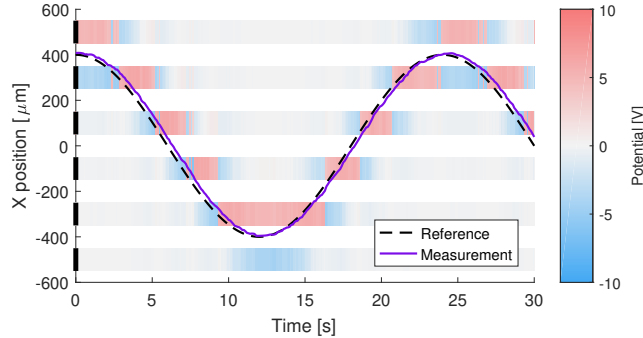


FIG. 7. Experimental verification of the proposed model of DEP in an experiment where a microparticle is steered along a reference trajectory. Only the transverse coordinate (i.e. x) is shown. The colors at electrode locations show what potentials were applied to the electrodes at a given time. Any vertical line shows what potentials were applied to the electrodes at the corresponding time.

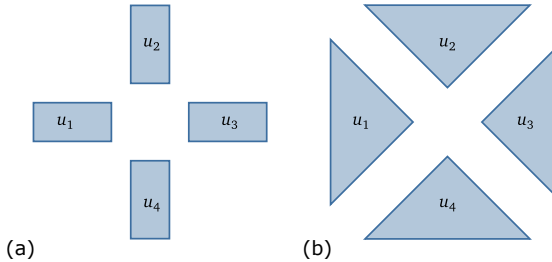


FIG. 8. Some other electrode array designs in the literature^{6,15} for which the proposed modeling methodology is also applicable.

useful when modeling general 2D (planar) electrode arrays (hence the solution domain is 3D) because some more accurate analytical approximations of the potential on the domain boundary (in the interelectrode gaps and outside the electrode array) such as polynomial or even linear do not seem to admit a closed-form solution of the integral giving the solution of the approximating boundary value problem.

ACKNOWLEDGMENTS

This research was funded by the Czech Science Foundation within the project P206/12/G014 (Centre for advanced bioanalytical technology, <http://www.biocentex.cz>).

- ¹H. A. Pohl, “Some effects of nonuniform fields on dielectrics,” *Journal of Applied Physics* **29**, 1182–1188 (1958).
- ²H. A. Pohl and I. Hawk, “Separation of living and dead cells by dielectrophoresis,” *Science* **152**, 647–649 (1966).
- ³R. Pethig, “Review article—dielectrophoresis: Status of the theory, technology, and applications,” *Biomicrofluidics* **4**, 022811 (2010).
- ⁴T. B. Jones, “Basic theory of dielectrophoresis and electrorotation,” *Engineering in Medicine and Biology Magazine, IEEE* **22**, 33–42 (2003).
- ⁵J. Žemánek, T. Michálek, and Z. Hurák, “Feedback control for noise-aided parallel micromanipulation of several particles using dielectrophoresis,” *Electrophoresis* **36**, 1451–1458 (2015).
- ⁶M. Kharbouly and M. Gauthier, “High speed closed loop control of a dielectrophoresis-based system,” in *Robotics and Automation (ICRA), 2013 IEEE International Conference on* (IEEE, 2013) pp. 1446–1451.
- ⁷M. Kharbouly, A. Melis, A. Bolopion, N. Chaillet, and M. Gauthier, “2d robotic control of a planar dielectrophoresis-based system.” in *Conference on the Manipulation, Manufacturing and Measurement on the Nanoscale, 3M NANO’12*. (2012) pp. 6–pages.

⁸B. Edwards and N. Engheta, "Electric tweezers: negative dielectrophoretic multiple particle positioning," *New Journal of Physics* **14**, 063012 (2012).

⁹K. V. Kaler and T. B. Jones, "Dielectrophoretic spectra of single cells determined by feedback-controlled levitation," *Biophysical journal* **57**, 173–182 (1990).

¹⁰N. Maresi, A. Romani, G. Medoro, L. Altomare, A. Leonardi, M. Tartagni, and R. Guerrieri, "A cmos chip for individual cell manipulation and detection," *IEEE Journal of Solid-State Circuits* **38**, 2297–2305 (2003).

¹¹H. Morgan, A. G. Izquierdo, D. Bakewell, N. G. Green, and A. Ramos, "The dielectrophoretic and travelling wave forces generated by interdigitated electrode arrays: analytical solution using fourier series," *Journal of Physics D: Applied Physics* **34**, 1553 (2001).

¹²D. E. Chang, S. Loire, and I. Mezić, "Closed-form solutions in the electrical field analysis for dielectrophoretic and travelling wave inter-digitated electrode arrays," *Journal of Physics D: Applied Physics* **36**, 3073 (2003).

¹³X. Wang, X.-B. Wang, F. F. Becker, and P. R. Gascoyne, "A theoretical method of electrical field analysis for dielectrophoretic electrode arrays using green's theorem," *Journal of physics D: applied physics* **29**, 1649 (1996).

¹⁴M. P. Hughes, *Nanoelectromechanics in engineering and biology* (CRC press, 2010).

¹⁵M. Kharbouthly, M. Gauthier, and N. Chaillet, "Modeling the trajectory of a microparticle in a dielectrophoresis device," *Journal of Applied Physics* **106**, 114312 (2009).

¹⁶L. C. Evans, *Partial Differential Equations*, 2nd ed. (American Mathematical Society, Providence, R.I, 2010).

¹⁷J. Zemánek, J. Drs, and Z. Hurák, "Dielectrophoretic actuation strategy for micromanipulation along complex trajectories," in *2014 IEEE/ASME International Conference on Advanced Intelligent Mechatronics* (IEEE, 2014) pp. 19–25.